IAC-20-C1.1.13

# Decentralized Electromagnetic Control of ChipSats Swarm Using Magnetorquers

**Danil Ivanov[a]*, Uliana Monakhova[b], Rui Gondar[c], Anna Guerman[d]**

[a] Space Systems Dynamics Department, Keldysh Institute of Applied Mathematics, RAS, Russian Federation, danilivanovs@gmail.com
[b] Space Systems Dynamics Department, Keldysh Institute of Applied Mathematics, RAS, Russian Federation, monakhova@phystech.edu
[c] University of Beira Interior, Covilha, Portugal, rui.mgg@hotmail.com
[d] C-MAST Center for Mechanical and Aerospace Science and Technology, University Beira Interior, Covilha, Portugal, anna@ubi.pt

* Corresponding Author

**Abstract**

A swarm of ChipSats equipped with miniature magnetorquers is considered. ChipSat is a satellite printed on 3.5 x 3.5 cm circuit board with set of sensors, solar panel, onboard computer and communication system. Assuming the relative motion between each satellite is known a decentralized Lyapunov-based control algorithm for a swarm of ChipSats is proposed in this study. Centralized and decentralized approaches are implemented. For centralized approach a CubeSat is assumed as main satellite and produce a high value of the magnetic torque, the surrounding ChipSats are implement such magnetic dipole moments in order to stop the drift. In case of decentralized approach the ChipSats select a pair and the relative drift between the ChipSats are stopped. During the motion the pairs members change and in such a way the relative drifts between all the satellites are set to zero vicinity. The proposed control schemes performance is studied numerically with different algorithm and ChipSats parameters.
**Keywords:** formation flying, swarm, ChipSats, electromagnetic control, magnetorquers

## 1. Introduction

New approaches to space exploration have motived extensive research and development of multi-satellite systems in an attempt to distribute and enhance the capabilities of monolithic spacecrafts. These complex systems consist of several smaller units, flying at short relative distances from one another or in similar orbits, working simultaneously towards the same task. Small satellite formations offer new scientific and commercial applications due to the increasing capability of its low-power micro components, flexible modular design and tolerance for individual unit failure. From an economic standpoint, smaller satellites are far more easy and cheaper to manufacture and launch into orbit than its larger counterparts. The overall performance of the formation can be improved throughout subsequent launches and maintained over time by replacing malfunctioning or damaged units. The development of nano- and picosatellites has led to the emergence of a new class of flying formation, referred to as "swarms" – numerous near-flying satellites moving along bounded relative trajectories. Swarms provide a set of capabilities in order to satisfy the mission requirements. However, the miniaturization of each unit poses limitations on autonomous control and inter-satellite communication. The swarm units can be controlled using centralized or decentralized approach. A centralized approach implies a "chief" satellite leading the formation, while the remaining "deputy" satellites monitor its motion and correct their own relative trajectories accordingly. This approach may be inadequate for large swarms due to limited tracking range and limited communication links. If the leader flies out of range or suffers critical system failure, the formation is at risk. With a decentralized approach, each unit controls its own relative motion, based on motion information of neighbour satellites, while avoiding communicational overload.

Relative motion determination is a key feature for successful formation flight. The state vectors of neighbouring satellites may be determined through different measurement methods such as image processing, astronomical interferometry (e.g. telescopes, radio waves, lasers) or GPS tracking. Once the absolute position of a satellite in the Earth-fixed inertial reference frame is determined, the difference between the absolute position vectors can be calculated. Astronomical interferometry technology requires expensive and sizeable components as well as high attitude accuracy, which can be challenging for low-cost missions with miniaturized vehicles. In the CanX-4&5 missions [1], primarily launched in 2014, relative navigation was achieved through carrier-phase differential GPS receivers to perform controlled, autonomous formations, with separations ranging from

1km to 50m, using a cold-gas propulsion system for relative motion control. The experimentally obtained relative position errors were below 2m, with the aid of attitude/position control algorithms as well as an extended Kalman filter running on-board. Image processing may also be used for relative position and attitude estimation using CCD optical sensors [2], which can be significantly reduced in sized, to track artificial markers (e.g. Light Emission Diodes (LEDs), corner-cube reflectors (CCR)) using on-board image processing software, allowing real-time translational/rotational motion tracking within the formation. As demonstrated in the PRISMA mission [3,4], an optical sensor provides "line-of-sight" measurements, exposing and isolating a single target from a limited distance, estimating its relative position and attitude. The navigation filter estimates the trajectory of the follower satellite, relative to the target (leader), by using projective geometry equations in image processing algorithm.

One of the main concerns when designing a flying formation mission is the implementation of autonomous relative motion control, to maintain the required spatial configuration of the satellites, manoeuvring to a desired relative orbit and correcting natural occurring relative drift. The common approach is the application of a 3-axis onboard propulsion system, allowing unrestricted thrust direction. If the number of thrusters is limited, and thrust direction cannot be arbitrarily changed, a single-input control approach is also feasible, assuming the thrust vector is fixed to the body reference frame. As studied in article [5], if the satellite is equipped with a passive magnetic attitude control system stabilizing the longitudinal axis along the local geomagnetic field, a single-input control is able to achieve bounded relative trajectories with two satellites in near circular orbit, depending on orbital parameters and initial conditions. As miniaturized satellites have unavoidable constraints on size, mass and energy and budget conventional propulsion systems may not be used for relative motion control. Alternative approaches have been proposed in recent years to develop effective, self-sufficient methods for motion control without propellant consumption using Aerodynamic Drag force and Solar Radiation Pressure. Yet both require sails onboard or satellite specific form-factors with high area-to-mass ratios [6–11]. Conventional propulsion systems require continuous fuel expenditure to maintain formation geometry, if a satellites' reserves are depleted its functionality will be compromised. Additionally, the risk of thruster plumes destabilizing the trajectories of neighbour spacecrafts, or "blinding" optical or thermal instruments on-board, makes fuel-dependent propulsion undesirable for swarm formations.

The paper from MIT's Space System's Laboratory [12] proposes the use of electromagnetic force between spacecrafts to control formation geometry. In Electromagnetic Formation Flight (EMFF) it is possible to control and maintain relative separation, relative attitude, and inertial rotation, which are critical manoeuvres for formation flying systems. This can be achieved using three orthogonal superconducting coils coupled with reaction wheels. The electrical current needed to generate the magnetic field can be converted from solar radiation through solar cells mounted on a satellite. Further studies on EMFF [10,11] address the performance of electromagnetic force in Low-Earth Orbits (LEO) with an adaptative control approach to nonlinear relative translational motion and attitude dynamics intended to compensate disturbances caused by the Earth's magnetic field. For an arbitrary N-satellite formation [10], a hybrid system is proposed with centralized translational control and decentralized attitude control.

A survey on active magnetic control algorithms [15] gives an in-depth analysis on the possible application methods for solely magnetic attitude control for small satellites. Article [16] describes a preliminary design of a femtosatellite prototype featuring an active 3-axial attitude control system using miniaturized orthogonal magnetorquers. For the magnetorquers, a two custom-build iron-core magnetorquer and air-core coil were designed to fit the 3.3 x 3.3 x 0.5 cm form-factor of the ChipSat. They are usually used as actuators for the attitude control. Interaction of the magnetic dipole moment with the Earth's magnetic field produces necessary torque acting on the satellite. The attitude motion is estimated using processing of measurements of the onboard sensors such as magnetometer and angular velocity sensor.

The present article addresses autonomous relative translational and attitude motion control of a femtosatellite swarm, composed of 3.3 x 3.3 x 0.5 cm satellites with 10g of mass, equivalent to the prototype proposed in article [16], considering the same method of deployment as was used for the Kicksat-2 mission. The custom miniature magnetorquers are the sole actuators, it has limit on dipole magnetic moment and consequently the dipole-to-dipole interaction force is also limited. It requires extremely short operating distances between satellites (from several meters up to several centimetres) for active translational control. This limitation is considered and the constraints on initial conditions after deployment are analysed as well. Each satellite in the swarm requires information about the relative motion of other satellites for control calculation. Relative navigation is challenging for a large swarm due to hardware limitations and limited inter-satellite communication links caused by frequency restrictions. Assuming each satellite can estimate the relative motion of the satellites in close proximity through an on-board relative navigation system, the decentralized control algorithm is applied to eliminate relative drift and to

achieve bounded relative trajectories. Due to the limited area of communication and limited effective range for magnetic force application the proposed algorithm takes a pair-to-pair approach to magnetic control. The construction and maintenance of the swarm is achieved by periodically linking nearby satellites in interchangeable pairs based on relative motion, applying the dipole-to-dipole interaction force as required and considering disturbances on neighbour units. The performance of the proposed control algorithm is studied numerically.

## 2. Motion equations

### *2.1 Undisturbed Motion Equations*

The Hill-Clohessy-Wiltshire (HCW) equations are utilized to describe the relative motion of two arbitrarily chosen satellites within the swarm [17], in a leader-follower system expressed in the rotating Hill reference frame. These linearized ordinary differential equations of free motion can be solved analytically. A complete solution is the sum of solution of the homogeneous equation, representing the effects on initial conditions and of a particular solution representing the effects of the applied forces, where the electromagnetic control force is later applied. The equations are valid for small relative distances, therefore the relative distance between the leader and follower must be several times of order smaller than the orbital radius of the leader.

Let $\mathbf{r}_i = (x_i, y_i, z_i)$ and $\mathbf{r}_j = (x_j, y_j, z_j)$ be the vectors of the i-th and j-th satellites in the reference frame, $i \neq j, i = 1,..., N, j = 1,..., N,$ where $N$ is the number of the satellites in the swarm. Then the components of the relative position vector $\mathbf{r}_{ij} = \mathbf{r}_j - \mathbf{r}_i = (x_{ij}, y_{ij}, z_{ij})$ in the case of a free motion are governed by the following equations

$$\begin{aligned} &\ddot{x}_{ij} + 2\omega\dot{z}_{ij} = 0, \\ &\ddot{y}_{ij} + \omega^2 y_{ij} = 0, \\ &\ddot{z}_{ij} - 2\omega\dot{x}_{ij} - 3\omega^2 z_{ij} = 0. \end{aligned} \tag{1}$$

The solution of the equations is as follows:

$$\begin{aligned} &x_{ij}(t) = -3C_1^{ij}\omega t + 2C_2^{ij}\cos(\omega t) - 2C_3^{ij}\sin(\omega t) + C_4^{ij}, \\ &y_{ij}(t) = C_5^{ij}\sin(\omega t) + C_6^{ij}\cos(\omega t), \\ &z_{ij}(t) = 2C_1^{ij} + C_2^{ij}\sin(\omega t) + C_3^{ij}\cos(\omega t), \end{aligned} \tag{2}$$

Where $C_1^{ij},...,C_6^{ij}$ are constants that depend on the initial conditions at $t = 0$:

$$\begin{aligned} &C_1^{ij} = \frac{\dot{x}_{ij}(0)}{\omega} + 2z_{ij}(0), C_2^{ij} = \frac{\dot{z}_{ij}(0)}{\omega}, C_3^{ij} = -3z_{ij}(0) - \frac{2\dot{x}_{ij}(0)}{\omega}, \\ &C_4^{ij} = x_{ij}(0) - \frac{2\dot{z}_{ij}(0)}{\omega}, C_5^{ij} = \frac{\dot{y}_{ij}(0)}{\omega}, C_6^{ij} = y_{ij}(0). \end{aligned} \tag{3}$$

The term responsible for the relative drift is $-3C_1^{ij}\omega t$. The relative trajectory of two satellites is closed if and only if $C_1^{ij} = 0$. However, ideal initial conditions for a closed free motion cannot be achieved. Moreover, perturbations and nonlinear effects induce additional relative drift between the satellites. Therefore, the satellites must be controlled to eliminate the drift and to achieve the bounded relative trajectory. Examples of the relative trajectories demonstrating the relative drift are presented in Fig. 1.

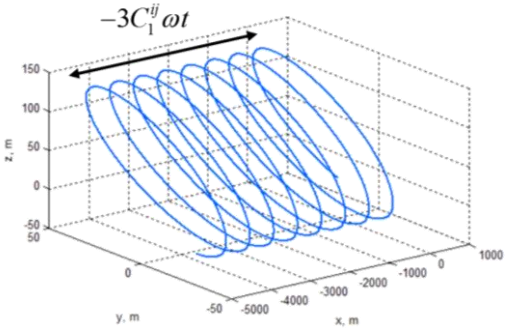


Fig. 1. Trajectories describing the relative drift

### *2.2 Controlled motion equations*

As previously mentioned, the electromagnetic force is considered for the control of the EMFF. This attraction force originates from the interaction of the magnetic dipoles generated by the 3-axial orthogonal magnetorquers of each satellite in the swarm when active. Considering a leader-follower system, the electromagnetic force acting on one of the satellites can be written as [18]:

$$\begin{aligned} \mathbf{f}_{ij} = -\frac{3m_0}{4\pi}\Bigg(-\frac{\mathbf{m}_j\cdot\mathbf{m}_i}{r^5}\mathbf{r}_{ij} - \frac{\mathbf{m}_j\cdot\mathbf{r}_{ij}}{r^5}\mathbf{m}_i - \frac{\mathbf{m}_i\cdot\mathbf{r}_{ij}}{r^5}\mathbf{m}_j + ... \\ ... + 5\frac{(\mathbf{m}_j\cdot\mathbf{r}_{ij})(\mathbf{m}_i\cdot\mathbf{r}_{ij})}{r^7}\mathbf{r}_{ij}\Bigg), \end{aligned} \tag{4}$$

where $\mathbf{m}_i$ and $\mathbf{m}_j$ are the dipole vectors of the leader and follower respectively, $r = |\mathbf{r}_{ij}|$ and $m_0 = 4\pi\cdot 10^{-7}\,\frac{H}{m}$ is the permeability of free space.

Consider the controlled motion equations of a swarm. Since the control is implemented to eliminate relative drift along the $Ox$ axis, acceleration vector $\mathbf{u}_{ij} = \mathbf{u}_j - \mathbf{u}_i = (u_x^{ij}, u_y^{ij}, u_z^{ij})$ has a non-zero component along the $Ox$ axis only, i.e. $u_y^{ij} = u_z^{ij} = 0$. Let $u_{ij} = u_x^{ij} = f_{ij}/m$ where $m$ is the mass of the satellite. Then the relative motion equations for i-th and j-th satellites are as follows:

$$\begin{aligned} &\ddot{x}_{ij} + 2\omega\dot{z}_{ij} = u_{ij}, \\ &\ddot{y}_{ij} + \omega^2 y_{ij} = 0, \\ &\ddot{z}_{ij} - 2\omega\dot{x}_{ij} - 3\omega^2 z_{ij} = 0. \end{aligned} \tag{5}$$

The considered drag force has no effect on the motion along *Oy* axis, it is defined only by the initial conditions after the launch. That is why the planar motion of the satellites in *Oxz* plane is considered in the paper.

*2.3 Angular motion equations*

Rigid satellite angular motion is considered. The satellite is equipped with three mutually orthogonal magnetorquers and three axis magnetometer. Euler's equations for the satellite with inertia tensor **J** are as follows:

$$\mathbf{J}\dot{\boldsymbol{\omega}} + \boldsymbol{\omega} \times \mathbf{J}\boldsymbol{\omega} = \mathbf{M} \tag{6}$$

where $\boldsymbol{\omega}$ is the absolute angular velocity vector in the body-fixed reference frame, $\mathbf{M}$ is the sum of the torques acting on the satellite. The torque may contain control part $\mathbf{M}_{ctrl}$ and disturbing part. The latter is divided into gravitational and interaction with magnetic field of Earth. Euler's equations are supplemented with kinematic relations. In simulation a quaternion is used to describe the satellite attitude. The kinematic relations are as follows:

$$\dot{\boldsymbol{\Lambda}} = \frac{1}{2}\mathbf{C}\boldsymbol{\Lambda}, \tag{7}$$

where $\boldsymbol{\Lambda}$ is quaternion,

$$\mathbf{C} = \begin{bmatrix} 0 & \omega_3 & -\omega_2 & \omega_1 \\ -\omega_3 & 0 & \omega_1 & \omega_2 \\ \omega_2 & -\omega_1 & 0 & \omega_3 \\ -\omega_1 & -\omega_2 & -\omega_3 & 0 \end{bmatrix}$$

and $\omega_i$ are the components of $\boldsymbol{\omega}$.

Control torque is $\mathbf{M}_{ctrl} = \mathbf{m}_{ctrl} \times \mathbf{B}$ where $\mathbf{m}$ is the dipole control moment of the satellite, $\mathbf{B}$ is the geomagnetic induction vector. Consider the B-dot control law for the satellite stabilization in the orbital reference frame

$$\mathbf{m}_{ctrl} = k\left(\boldsymbol{\omega} \times \mathbf{B}\right) \tag{8}$$

where $k > 0$ is the positive control parameters, $\mathbf{B}$ is the geomagnetic induction vector. Gravitational torque is

$$\mathbf{M}_{gr} = 3\omega_0^2 \mathbf{e}_3 \times \mathbf{J}\mathbf{e}_3 \tag{9}$$

where $\mathbf{e}_3$ is the satellite unit radius-vector in the body-fixed reference frame.

Other disturbing source $\mathbf{M}_{\oplus} = \mathbf{m} \times \mathbf{B}_{\oplus}$ is torque related to the force of magnetic interaction with Earth, where $\mathbf{m}$ is the dipole moment of the satellite, $\mathbf{B}_{\oplus}$ is the Earth's geomagnetic induction vector. Considering all the listed torques acting on the satellite, Euler's equations can be represented as follows:

$$\mathbf{J}\dot{\boldsymbol{\omega}} + \boldsymbol{\omega} \times \mathbf{J}\boldsymbol{\omega} = \mathbf{M}_{ctrl} + \mathbf{M}_{gr} + \mathbf{M}_{\oplus} \tag{10}$$

## 3. Lyapunov-based control algorithm

The control goal is to construct and maintain a swarm of satellites eliminating their relative drift. The shape and size of relative trajectories are determined by the values $C^{ij}$ from (3). Henceforth the constant values $C^{ij}$ of the free relative motion (1) are considered as changing for the controlled motion equations (5). From the motion equations (2) it is concluded that the constants $C_1^{ij}$ are responsible for the drift. The control is aimed to eliminate the relative drift $C_1^{ij}$. The following Lyapunov candidate function is constructed:

$$V = \frac{1}{2}(C_1^{ij})^2, \tag{11}$$

The conditions $V > 0,\ V(0) = 0$ are satisfied. The derivative of the Lyapunov function should be negative to satisfy the Barbashin-Krasovskii theorem [19] to achieve the global asymptotical stability. The derivative is as follows:

$$\dot{V} = C_1^{ij}\dot{C}_1^{ij} = C_1^{ij}\left(\frac{\ddot{x}^{ij}}{\omega} + 2\dot{z}^{ij}\right). \tag{12}$$

Regroup the expression and demand that Lyapunov function be a definite negative function

$$\dot{V} = \frac{1}{\omega}C_1^{ij}(\ddot{x}^{ij} + 2\omega\dot{z}^{ij}) = C_1^{ij}\frac{1}{\omega}u_x = -\frac{k}{\omega}\left(C_1^{ij}\right)^2 \tag{13}$$

where $k > 0$. The resulting control law is

$$u^{ij} = -kC_1^{ij}. \tag{14}$$

The control $u_{ij}$ provides a convergence to a closed relative trajectory. The developed control law (14) is similar to the PD controller.

*3.1 Centralized control approach*

In the centralized approach (Fig.2) there is a satellite acting as a 'leader' of the group, i.e. tracking positions of 'subordinate' satellites to make control decisions based on this information. It is assumed that 3U CubeSat is a leader of ChipSats and knows their relative positions. Also CubeSat performing constant maximum value of magnetic dipole that can be produced by its magnetorquers is considered.

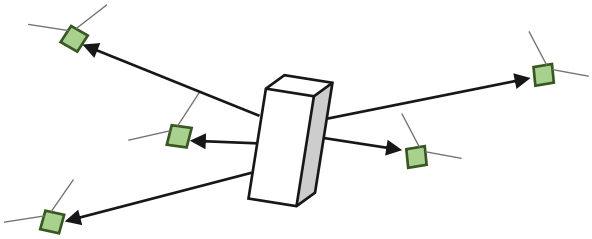

Fig.2. Centralized approach

In the first step of control application the $C_1^{1i}$ between leader and i-th satellite (ChipSat) is counted according to initial conditions after the launch. Then the

value of required control $u^{1i}$ (14) for the i-th satellite can be found. Knowing the dipole moment of the leader and required control $u^{1i}$, the dipole moment $\mathbf{m}_i$ for the i-th satellite is counted using the equations of magnetic interaction (4). The value of dipole moment that can be produced is limited by technical capabilities of ChipSat's magnetorquers. Therefore if $|\mathbf{m}_i| > m_{\max}$ the required value of control only partially can be performed.

*3.2 Decentralized control approach*

With a decentralized approach, each satellite controls its own relative motion, based on motion information of the most neighbouring satellite (Fig.3).

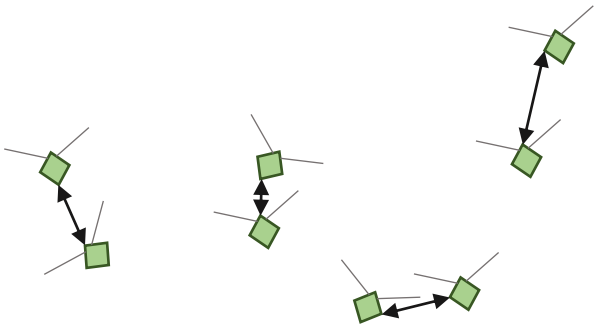

Fig.3. Decentralized approach

In the first step of control application the $C_1^{ij}$ between i-th and j-th satellite, which are the nearest to each other, is counted according to initial conditions after the launch. Then the value of required control $u^{ij}$ (14) for the i-th satellite can be found. Further, the j-th satellite produce its maximum value of dipole moment, knowing this value and required control $u^{ij}$, the dipole moment $\mathbf{m}_i$ for the i-th satellite is counted using the equations of magnetic interaction (4). In this approach the value of dipole moment that can be produced is also limited, therefore if $|\mathbf{m}_i| > m_{\max}$ the required value of control only partially can be performed.

## 4. Numerical study

Consider a swarm of the ChipSats launched by CubeSat in low Earth Orbit. Each ChipSat is equipped with three orthogonal magnetorquers and capable to produce the required magnetic dipole moment that is not exceed defined maximal value. In case the required magnetic dipole is more that can be implemented then the maximal value is produced. All the simulation parameters values are listed in Table 1.

Table 1. Simulation parameters

| | |
|---|---|
| Main parameters of the swarm | |
| Number of satellites in the swarm, $N$ | 20 |
| Initial conditions | |
| Initial relative drift, $C_1$ | rand([-0.1;0.1]) m |
| Initial relative position constants $C_2 - C_6$ | rand([-0.1;0.1]) m |
| ChipSats parameters | |
| Mass of the ChipSat, $m$ | 10g |
| Inertia tensor for ChipSat, $\mathbf{J}_{ChipSat}$ | diag (8, 8, 15)·10$^{-7}$ kg·m$^2$ |
| Inertia tensor for CubeSat, $\mathbf{J}_{CubeSat}$ | diag (5, 25, 25)·10$^{-3}$ kg·m$^2$ |
| Maximal magnetic dipole value of magnetorquers, $m_{\max}$ | 0.01 Am$^2$ |
| Orbital parameters | |
| Orbit altitude, $h$ | 500 km |
| Orbit inclination, $i$ | 51.7° |
| Algorithms parameters | |
| Minimal distance for the satellite pairing | 0.05 m |
| Maximal distance for the satellite pairing | 1 m |
| Value of the relative drift when the satellites are not control | 0.01 m |

*4.1. Free motion of the swarm*

Initially, The ChipSats has random initial conditions, their positions are in the certain vicinity of the origin of the reference frame, and the values and directions of the relative velocity vectors are arbitrary. Due to this random initial condition after the launch the relative motion is not bounded. Fig. 4. presents the trajectories of the free motion of the 20 ChipSats relative to the first satellite. The relative distances are gradually increase according to Fig. 5. This unbounded motion is caused by the relative drift due to random initial conditions, the drift parameters $C_1$ is presented in Fig. 6.

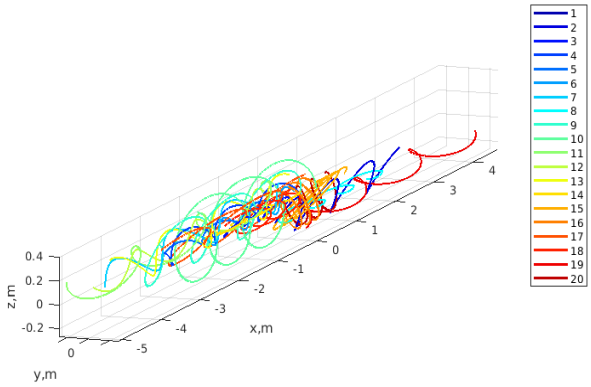


Fig. 4. Relative trajectories of the swarm free motion

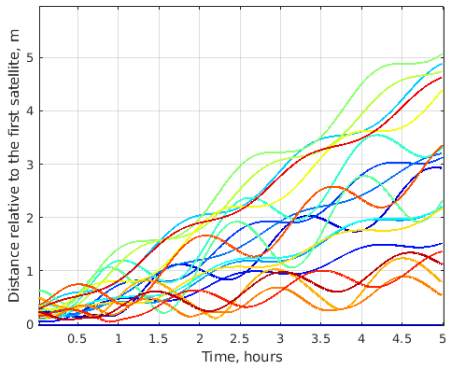


Fig. 5. Distances relative to the first satellite

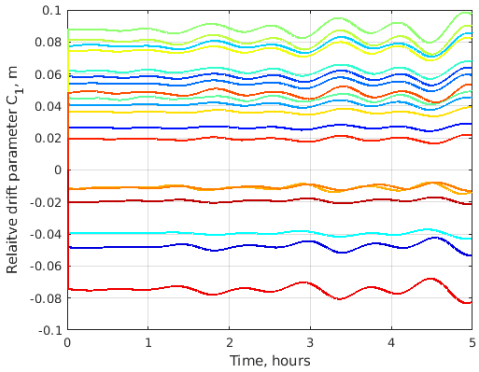


Fig. 6. Relative drifts in case of free motion

*4.2 Controlled motion examples for decentrelized approach*

Consider an application of the proposed control algorithm for the same initial conditions as described for the example of free relative motion. First, the decentralized pairing strategy based on the closest satellite with nonzero relative drift is demonstrated. The Fig. 7. shows the relative trajectories of the satellites after the application of the control algorithm. From Fig. 8 and 9 it can be concluded that the relative drift is stopped after 0.5 hours and the relative trajectories become bounded.

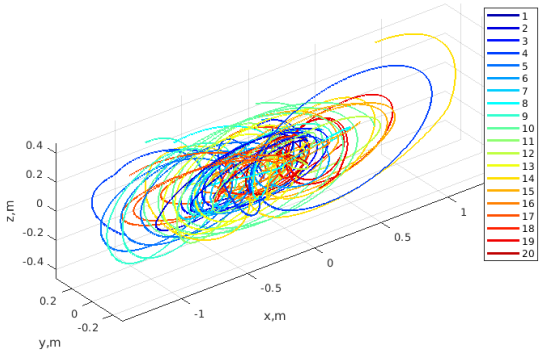


Fig. 7. Relative trajectories

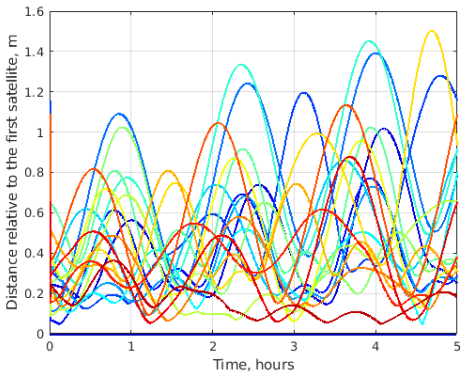


Fig. 8. Distances relative to the first satellite

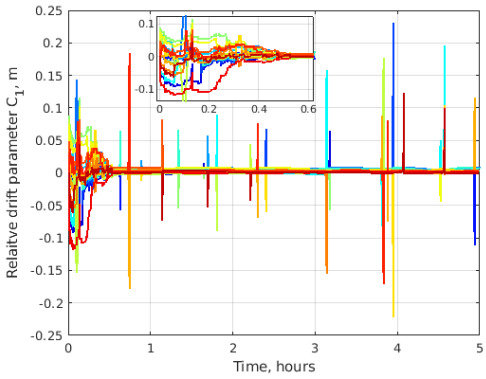


Fig. 9. Relative drifts

Fig. 10 demonstrates the paired satellites over the time during the simulation: the y-axis defines the satellite number and the star sign color correspond to the paired satellite. It can be seen that the paired satellites are changing with time and it allows to stop the relative drift between all of the satellites in the end. After 1 hour the satellites are mostly not paired, since the drift is stopped. But randomly after the collision avoidance application when the drift is high enough the control for the stopping drift is applied again and the satellites are paired seldom. A set of peaks in the Figure 9 in the relative drifts are caused by the collision avoidance control application. The temporary high relative drift quite rapidly decreases to zero vicinity by the control applications.

Fig. 11 and 12 demonstrate the magnetic dipole moments of all of the satellites and the produced electromagnetic forces. The magnetic dipoles values do not exceed the maximal value of 0.01 $Am^2$. The produced force at the peak reaches the value of $3 \cdot 10^{-7}$ N. The peaks after swarm construction are caused by the collision avoidance control.

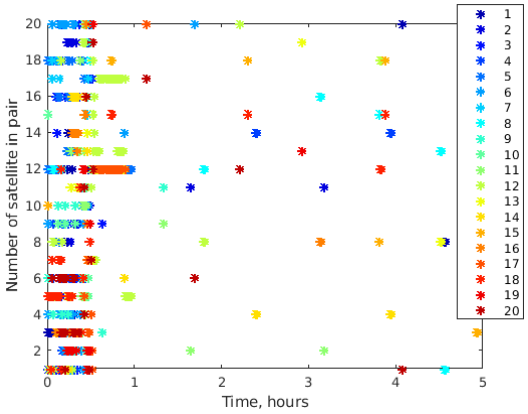


Fig. 10. The pairing of the satellites over the time

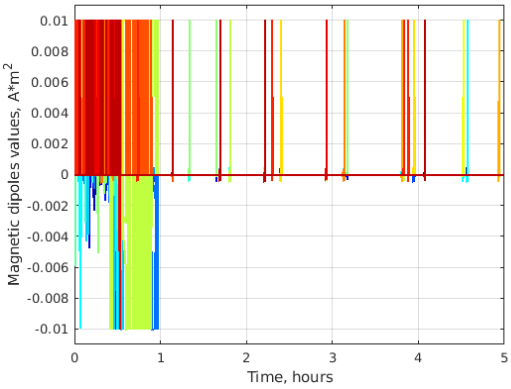


Fig. 11. Values of the magnetic dipole moments of all the satellites

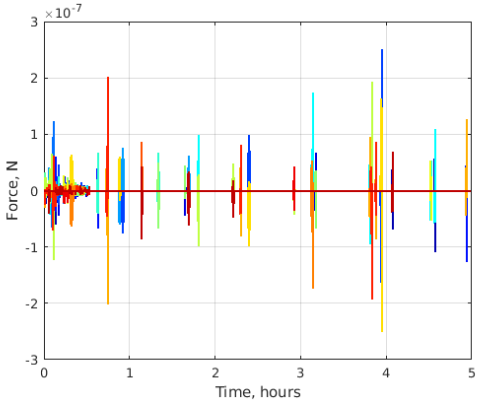


Fig. 12. Produced electromagnetic forces

When the satellites are not paired and do not involved in the translational motion control the angular velocity damping algorithm is applied. The dipole-to-dipole magnetic interaction result in torque that affects the angular motion and it leads to increase of the angular momentum. Fig. 13 demonstrates the angular velocity components of all of the satellites in the swarm and Fig. 14 the quaternion components of all the satellites. During active relative drift control the satellites angular rate increases up to 1000 deg/s that approximately equal to 3 rotations per second, that is quite high value. Nevertheless, when the satellite is not paired the angular velocity damping by the magnetorquers decreases these values quite rapidly during a set of minutes. After 1 hour when the relative drift is stopped the angular velocity is close to zero. Seldom the collision avoidance control increases the angular velocity up to 100 deg/s but this angular motion is damped afterward as well.

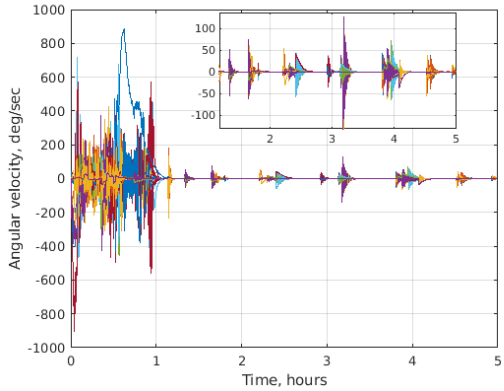


Fig. 13. Angular velocity vector components of all the satellites

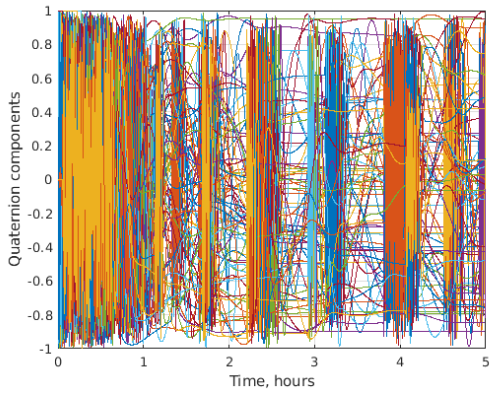


Fig. 14. Quaternion components of all the satellites

*4.3 Controlled motion examples for centrelized approach*

Consider an application of the centralized control algorithm for the same initial conditions as described for previous example except number of satellites, $N = 12$ in this demonstration. The Fig. 15. shows the relative trajectories of the satellites after the application of the control algorithm. From Fig. 16 it can be concluded that the relative drift is stopped after several seconds and the relative trajectories become bounded.

Fig. 17 demonstrates the magnetic dipole moments of all of the satellites during the simulation. The magnetic dipoles values do not exceed the maximal value of 0.01 $Am^2$.

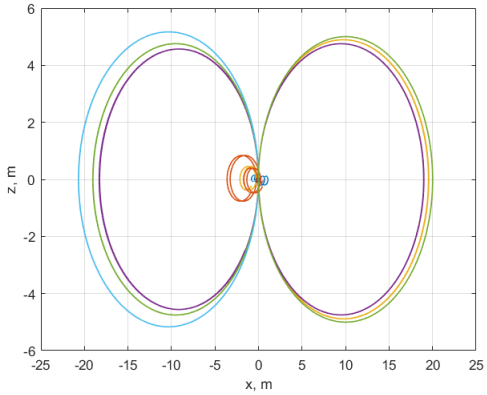


Fig. 15. Relative trajectories

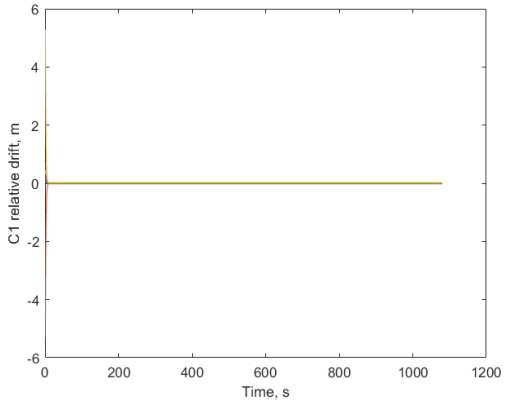


Fig. 16. Relative drifts

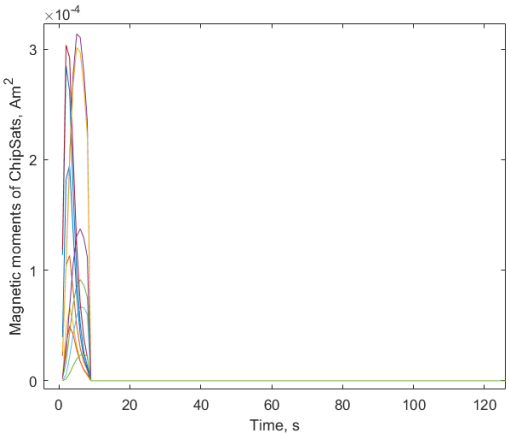


Fig. 17. Values of the magnetic dipole moments

When the satellites are involved in the translational motion control the angular velocity damping algorithm is applied to CubeSat. The dipole-to-dipole magnetic interaction result in torque that affects the angular motion and it leads to increase of the angular momentum. Fig. 18 demonstrates the angular velocity components of CubeSat. After 15 minutes when the relative drift is stopped the angular velocity becomes zero.

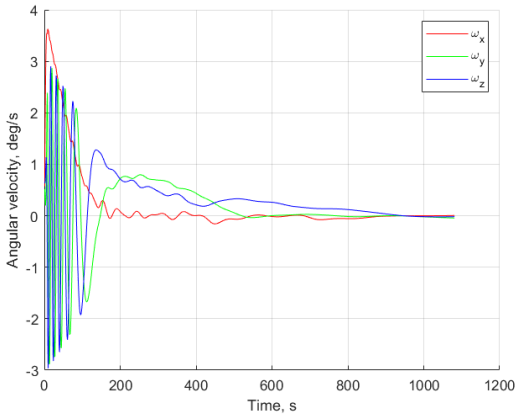


Fig. 18. Angular velocity vector components

## 5. Conclusions

Due to tiny size of ChipSats and extremely short relative distances the electromagnetic interaction stops the relative drift between satellites. Magnetorquers can be used both for translational control and angular velocity damping. Algorithm application performance strongly depends on a set of initial parameters.

## Acknowledgements

Portuguese Foundation for Science and Technologies via Centre for Mechanical and Aerospace Science and Technologies, C-MAST, POCI-01-0145-FEDER-007718.

## References

[1] N.H. Roth, B. Risi, R.E. Zee, Flight Results From the Canx-4 and Canx-5 Formation Flying Mission, in: Proceedings of International Workshop on Satellite Constillations and Formation Flying, June 19-21, 2017, CO, Bouldder, 2017: pp. 1–17.

[2] R. Opromolla, G. Fasano, G. Rufino, M. Grassi, A review of cooperative and uncooperative spacecraft pose determination techniques for close-proximity operations, Progress in Aerospace Sciences. 93 (2017) 53–72. doi:10.1016/J.PAEROSCI.2017.07.001.

[3] R. Noteborn, Flight Results from the PRISMA Optical Line of Sight Based Autonomous Rendezvous Experiment, in: Proceedings of the 4th International Conference on Spacecraft Formation Flying Missions an Technologies, May 2011, Montreal, Canada, 2011: p. 10.

[4] C. Chasset, R. Noteborn, P. Bodin, R. Larsson, B. Jakobsson, 3-Axis magnetic control: Flight results of the TANGO satellite in the PRISMA mission, CEAS Space Journal. 5 (2013) 1–17. doi:10.1007/s12567-013-0034-9.

[5] A. Guerman, M. Ovchinnikov, G. Smirnov, S.

Trofimov, Closed Relative Trajectories for Formation Flying with Single-Input Control, Mathematical Problems in Engineering. 2012 (2012) 1–20. doi:10.1155/2012/967248.

[6] S. Gong, G. Yunfeng, J. Li, Solar sail formation flying on an inclined Earth orbit, Acta Astronautica. 68 (2011) 226–239. doi:10.1016/j.actaastro.2010.08.022.

[7] S. Gong, H. Baoyin, J. Li, Solar Sail Formation Flying Around Displaced Solar Orbits, Journal of Guidance, Control, and Dynamics. 30 (2007) 1148–1152. doi:10.2514/1.24315.

[8] D. Ivanov, U. Monakhova, M. Ovchinnikov, Nanosatellites swarm deployment using decentralized differential drag-based control with communicational constraints, Acta Astronautica. 159 (2019) 646–657. doi:10.1016/J.ACTAASTRO.2019.02.006.

[9] D. Ivanov, U. Monakhova, A. Guerman, M. Ovchinnikov, D. Roldugin, Decentralized differential drag based control of nanosatellites swarm spatial distribution using magnetorquers, Advances in Space Research. (2020). doi:10.1016/j.asr.2020.05.024.

[10] D. Ivanov, M. Kushniruk, M. Ovchinnikov, Study of satellite formation flying control using differential lift and drag, Acta Astronautica. 145 (2018) 88–100. doi:10.1016/J.ACTAASTRO.2018.07.047.

[11] Y. Mashtakov, M. Ovchinnikov, T. Petrova, S. Tkachev, Two-satellite formation flying control by cell-structured solar sail, Acta Astronautica. 170 (2020) 592–600. doi:10.1016/j.actaastro.2020.02.024.

[12] E.M.C. Kong, D.W. Kwon, S.A. Schweighart, L.M. Elias, R.J. Sedwick, D.W. Miller, Electromagnetic formation flight for multisatellite arrays, Journal of Spacecraft and Rockets. 41 (2004) 659–666. doi:10.2514/1.2172.

[13] D.W. Miller, U. Ahsun, J.L. Ramirez-Riberos, Control of Electromagnetic Satellite Formations in Near-Earth Orbits, Journal of Guidance, Control, and Dynamics. 33 (2010) 1883–1891. doi:10.2514/1.47637.

[14] D.W. Kwon, Propellantless formation flight applications using electromagnetic satellite formations, Acta Astronautica. 67 (2010) 1189–1201. doi:10.1016/j.actaastro.2010.06.042.

[15] M.Y. Ovchinnikov, D.S. Roldugin, A survey on active magnetic attitude control algorithms for small satellites, Progress in Aerospace Sciences. 109 (2019) 100546 1–17. doi:10.1016/J.PAEROSCI.2019.05.006.

[16] N. Ireland, Z. Hu, T. Timmons, C. Mcinnes, Enlighten – Research publications by members of the University of Glasgow BIS-RS-2019-26 Development of a 10g Femto-satellite with Active Attitude Control, (2019) 12–14.

[17] G.W. Hill, Researches in Lunar Theory, American Journal of Mathematics. 1 (1878) 5–26.

[18] C. Zhang, X.L. Huang, Angular-momentum management of electromagnetic formation flight using alternating magnetic fields, Journal of Guidance, Control, and Dynamics. 39 (2016) 1292–1302. doi:10.2514/1.G001529.

[19] E.A. Barbashin, On construction of Lyapunov functions for non- linear systems, in: Proc. First Congr. IFAK, Moscow, 1961: pp. 742– 751.